NASA TECHNICAL MEMORANDUM

NASA TM X-68020

NASA TM X-68020

ANALYSIS OF A SUPERSONIC-COMBUSTION ROCKET CONCEPT

by Leo Franciscus
Lewis Research Center
Cleveland, Ohio
February, 1972

ANALYSIS OF A SUPERSONIC-COMBUSTION ROCKET CONCEPT

by Leo Franciscus

Lewis Research Center

E-6825

SUMMARY

A preliminary analysis has been made of a supersonic-combustion rocket engine concept using hydrogen and oxygen propellants. The ejector action of a separate small rocket motor is employed to pump the propellants to high stagnation pressures and supersonic velocities. Therefore complicated heavy turbopumps are eliminated and cooling problems of a sonic throat are reduced. The results of the study show that vacuum specific impulse levels as high as a conventional rocket having the same chamber pressure as the drive motor are possible. The supersonic-combustion rocket would be an attractive alternate for a high-altitude low-thrust conventional rocket operating with a pressure feed propellant system. It would also be a convenient technique for obtaining extremely high thrusts without the need for developing corresponding large turbopumps.

I. INTRODUCTION

Conventional rocket motors employing pump-fed liquid propellants have been in wide use for many years, and their design and development, while rarely trouble-free, can be considered to be basically applications of previous practice. Nevertheless, it would be desirable if means were available to simplify the heavy expensive turbopumps that are used to inject the propellant into the combustion chamber. This is especially the case if very large rockets are contemplated. Conversely, it is also the case for very small rockets where the complexity and expense of turbopumps cannot be justified. In this instance the pumps are usually discarded in favor of a pressure-fed system which then suffers the penalties of lower engine specific impulse and high tank weight.

In reference 1, Franciscus has studied the possibility of replacing the mechanical turbopumps by the ejector action of small auxiliary rockets (drive rockets). If the propellant heat sink is large enough to prevent vaporization of the propellant by the hot drive rocket gas large increases in propellant stagnation pressure may be possible. This requires mass ratios (ratio of propellant mass flow to drive rocket mass flow) from 50 to 100 for hydrogen and oxygen. At lower mass ratios vaporization occurs and pumping performance is greatly impaired. The present report studies an alternate concept proposed by

Richard J. Weber of NASA-Lewis that may be an improvement over the previous scheme.

In this concept small drive rockets are again used to pressurize the propellants via ejector action. However, for good pumping performance the propellants are allowed to vaporize and reach supersonic velocities in the combustor. The weight and complexity of the turbopumps are thus eliminated. Also the exhaust nozzle throat is eliminated. This in combination with much lower combustor temperatures and pressures eases cooling problems and may permit lighter structure. Three alternate schemes for a supersonic combustion rocket are shown in figure 1. In the first scheme, figure 1(a), the propellants are pumped by the ejector action of a small rocket located in the supply line of each propellant similar to the ejector pump discussed in reference 1. If the mass ratios (ratio of propellant mass flow to rocket mass flow) are less than 50 the propellants are vaporized by the hot exhaust gases of the drive rockets and leave the pumps at supersonic velocities. Considerable losses would be incurred by diffusing the propellants to subsonic velocities before introducing them into the combustor. Therefore, the propellants enter the combustor directly from the pumps and mix and burn at supersonic speeds. Since the propellants entering the combustor are at low temperature, an ignition source may be required in this scheme. In the second scheme, figure 1(b), the propellants are drawn into a mixing chamber before entering the combustor. The mixed propellants then enter the combustor where they are ignited by the drive rocket exhaust gas. The high velocity drive rocket gas also imparts momentum to the incoming mixture and the gases leave the combustor at supersonic speeds. The third scheme figure 1(c) is similar to the first one except that a single drive rocket draws the propellants into the combustor and the hot drive rocket gas may be used as an ignition source. In addition, the velocity of the propellants entering the combustor may not be supersonic but are accelerated to supersonic speeds before leaving the combustor. In all three schemes the gases leave the combustor at supersonic velocities; therefore, a sonic throat is not required. However a supersonic nozzle may be required for further expansion and improved performance.

The results of an analytical investigation of the third scheme are presented in this report. The study was confined to LOX/LH_2 propellants at a mixture ratio of 8 for both the drive rocket and main propellants. For a preliminary study of this nature a one-dimensional flow model was used in the analysis. Also, complete mixing and burning in the combustor were assumed, and shock and friction losses were not considered. The figure of merit used is the ideal vacuum specific impulse. Cycle parameters shown in Table I were varied to determine their effects on the vacuum specific impulse. Also, a number of combustor pressure distributions also given in Table I were studied to determine their effect on vacuum specific impulse.

II. SYMBOLS

A	cross sectional area, m^2; ft^2
g	gravitational constant, m/sec^2; ft/sec^2
h	enthalpy, cal/g; Btu/lb
I_{vac}	vacuum specific impulse, sec
J	mechanical equivalent of heat, N-m/J; 778 ft-lb/Btu
M	Mach number
m	molecular weight, gr/mole; lbm/mole
$\dot{m}$	mass flow rate kg/sec; slugs/sec
P	pressure, atm
R	universal gas constant, 8.31 J/mole K; 1545 ft-lbf/(mole)(^oR)
S	entropy, J/kg K; Btu/(slug)(^oR)
T	temperature, K; ^oR
V	velocity, m/sec; ft/sec
ρ	density, kg/m^3; $slugs/ft^3$

Subscripts

1	combustor entrance
2	combustor exit
e	nozzle exit
H	hydrogen
O	oxygen
P	drive rocket
T	total or chamber condition

III. METHOD OF ANALYSIS

The drive rocket gas enters the combustor at conditions specified by the drive-rocket chamber and static pressures, P_{TP} and P_P, and a mixture ratio of 8. The flow properties of the drive rocket (enthalpy, temperature and velocity) were determined from reference 2 assuming chemical equilibrium. The static pressures of the hydrogen and oxygen entering the combustor are assumed to be equal to P_P. The stagnation pressures of both propellants are assumed to be 415 kN/m^2. The oxygen is assumed to be a liquid at a temperature of 90 K (162° R). The hydrogen is assumed to be a gas with a stagnation temperature of 300 K (540° R). For a specified P_P, therefore, the flow properties of the oxygen and hydrogen may be determined.

The ratio of exit cross-sectional area to entrance cross-sectional area for the mixer/combustor is specified as an independent parameter. The solution for the combustor exit conditions for a specified area ratio is carried out by an iteration procedure for a specified mass ratio, $\dot{m}_S/\dot{m}_P$. The equation for conservation of momentum for the three streams entering the combustor is:

$$m_2V_2 + P_2A_2 = \dot{m}_PV_P + P_PA_P + \dot{m}_0V_0 + P_0A_0 + \dot{m}_HV_H + P_HA_H + \int_1^2 PdA \qquad (1)$$

The combustor entrance area is:

$$A_1 = A_P + A_H + A_0$$

It is assumed that the static pressures of the three streams entering the combustor are equal.

$$P_P = P_0 = P_H$$

The combustor pressure distribution as a function of area ratio is needed to evaluate the wall-pressure force term in equation (1). The form of the pressure distribution is affected by the rate of mixing and burning along the length of the duct and by the designer's selection of how cross-sectional area varies with length. Since a detailed study of this type is beyond the scope of this study the following pressure distributions as functions of area were chosen for investigation.

$$\text{Linear} - \int_1^2 P\,dA = \frac{P_1 + P_2}{2}(A_2 - A_1)$$

$$\text{Parabolic} - \int_1^2 P\,dA = \frac{P_1 + 2P_2}{3}(A_2 - A_1)$$

$$\text{Elliptic} - \int_1^2 P\,dA = \left[\left(1 - \frac{\pi}{4}\right)P_1 - \frac{\pi}{4}P_2\right](A_2 - A_1)$$

Equation (1) is then solved for V_2:

$$V_2 = V_P \frac{\dot{m}_P}{\dot{m}_2} + V_0 \frac{\dot{m}_0}{\dot{m}_2} + V_H \frac{\dot{m}_H}{\dot{m}_2} + \frac{P_P\, A_1/A_0\, \dot{m}_0/\dot{m}_2\, N}{\rho_0 V_0} \qquad (2)$$

where the form of N corresponds to one of the assumed pressure distributions as follows:

$$\text{Linear} - N = \frac{1}{2}(1 - P_2/P_1)(A_2/A_1 + 1)$$

$$\text{Parabolic} - N = \frac{1}{3}(1 - P_2/P_1)(A_2/A_1 + 2)$$

$$\text{Elliptic} - N = (1 - P_2/P_1)\left[\left(1 - \frac{\pi}{4}\right)A_2/A_1 + \pi/4\right]$$

The static enthalpy at the combustor exit is determined from conservation of energy:

$$h_2 = (h_P + V_P^2/2J)\ \frac{\dot{m}_P}{m_2} + (h_0 + V_0^2/2J\ )\ \frac{\dot{m}_0}{m_2} +$$

$$(h_H + V_H^2/2J\ + \Delta h)\ \frac{\dot{m}_H}{\dot{m}_2} - V_2^2/2J \qquad (3)$$

where Δh is the heat of combustion in calories per gram of hydrogen.

The static temperature, T_2, is determined from thermodynamic data of reference 2 using the products of combustion of hydrogen and oxygen in chemical equilibrium.

A second solution for V_2 is obtained from the equations of state and conservation of mass.

From the equation of state:

$$\rho_2 = \frac{P_2}{T_2 gR/m_2} \qquad (4)$$

From conservation of mass:

$$\dot{m}_2 = \dot{m}_P + \dot{m}_0 + \dot{m}_H$$

or

$$\frac{\dot{m}_2}{\dot{m}_0} = \frac{\dot{m}_P}{\dot{m}_0} + 1 + \frac{\dot{m}_H}{\dot{m}_0}$$

For a stoichiometric mixture then:

$$\frac{\dot{m}_2}{\dot{m}_0} = 1.125 + \frac{\dot{m}_P}{\dot{m}_0}$$

and $\dot{m}_P/\dot{m}_0$ can be determined from the prescribed mass ratio since $\dot{m}_S = \dot{m}_0 + \dot{m}_H$ so that

$$\dot{m}_2 = 1.125\ \dot{m}_0 \left(1 + \frac{1}{\dot{m}_S/\dot{m}_P}\right) \qquad (5)$$

The second solution for V_2 is then determined from equation (4).

$$V_2' = 1.125 \left(1 + \frac{1}{\dot{m}_S/\dot{m}_P}\right) \frac{\rho_0}{\rho_2} \frac{A_0}{A_2} V_0 \qquad (6)$$

where

$$\frac{A_2}{A_0} = \frac{A_2}{A_1} \left[1 + 1.125 \frac{\rho_0 V_0}{\rho_P V_P} \frac{1}{\dot{m}_S/\dot{m}_P} + 0.125 \frac{\rho_0 V_0}{\rho_H V_H}\right] \qquad (7)$$

Equations (2), (3), (4) and (6) are solved using corrected values of P_2 until $|V_2/V_2'| = .01$.

A special case of the preceding equations was considered in which the duct shape is selected such that mixing and combustion take place at constant pressure. In this case equation (1) becomes:

$$V_2 = V_P \frac{\dot{m}_P}{\dot{m}_2} + V_0 \frac{\dot{m}_0}{\dot{m}_2} + V_H \frac{\dot{m}_H}{\dot{m}_2} \qquad (8)$$

h_2 is determined from equation (3) and T_2 is found from thermodynamic data. ρ_2 is then found from equation (4). The combustor area ratio is:

$$\frac{A_2}{A_1} = \frac{A_2/A_0}{\left[1.0 + \frac{1.125\rho_0 V_0}{\rho_P V_P} \frac{\dot{m}_P}{\dot{m}_S} + 0.125 \frac{\rho_0 V_0}{\rho_H V_H}\right]} \qquad (9)$$

where

$$\frac{A_2}{A_0} = 1.125 \frac{\rho_0 V_0}{\rho_2 V_2} \left(1.0 + \frac{\dot{m}_P}{\dot{m}_S}\right)$$

The nozzle exit properties are determined assuming an isentropic expansion from P_2 to a specified exit pressure, P_e. Since S_2 is determined from P_2 and T_2, h_e and T_e are found from thermodynamic data. The nozzle exit velocity is:

$$V_e = [V_2^2 + 2J(h_2 - h_e)]^{1/2} \qquad (10)$$

The ideal vacuum specific impulse is

$$I_{vac} = \frac{V_e}{g} + \frac{R}{m_e}\frac{T_e}{V_e} \tag{11}$$

and the nozzle area ratio:

$$\frac{A_e}{A_2} = \frac{P_2}{P_e}\frac{V_2}{V_e}\frac{T_e}{T_2} \tag{12}$$

IV. RESULTS AND DISCUSSION

In the Method of Analysis section it was mentioned that the combustor pressure distribution must be defined in order to determine the gas properties at the combustor exit. The pressure distribution has a significant effect on the rocket performance. For the same area ratio and combustor exit pressure, higher pressure profiles result in higher combustor exit velocities, lower temperatures and higher specific impulse. However, the pressure distribution is dependent on many variables, i.e., the pressure, temperature and velocity of the drive rocket exhaust gas and the two propellants entering the combustor, the mass ratio and combustor area ratio and also the mixing and burning process in the combustor.

Defining the pressure distributions for the range of parameters considered here is beyond the scope of this study. Therefore, a number of pressure profiles as a function of combustor cross-sectional area were adopted for the purpose of showing this effect on the results of the study. Typical profiles for linear, parabolic, and elliptical pressure distributions for a combustor area ratio of 40 are shown in figure 2. For comparison the pressure distribution for an isentropic expansion from a sonic throat is also shown. A heat addition process would result in higher pressures than for an isentropic process. This is shown by the pressure at the combustor exit for all three pressure profiles being about 10 to 20 times higher than that for the isentropic process.

The simple case of constant-pressure mixing and burning (for which, of course, no assumption need be made of the combustor pressure distribution) is discussed first. The effect of the combustor pressure distribution on the vacuum specific impulse is then shown using the three pressure profiles mentioned. The parabolic profile is then selected and the effect of the parameters of Table I on vacuum specific impulse are shown. Except where noted the vacuum specific impulse was computed assuming the main engine nozzle expanded the gases to a nozzle exit pressure of .01 atmospheres.

Constant-Pressure Mixing and Burning

Table II shows the Mach numbers and velocities of the three streams entering the combustor for the range of drive rocket chamber and nozzle exit pressures considered. For all cases the drive gas Mach numbers are supersonic. The hydrogen Mach numbers range from 0.68 to 1.2 and the liquid oxygen velocities are low (13.75-19 m/S)(45-62 ft/sec). The drive gas imparts momentum to the secondary streams and, for specified P_{TP} and P_P, the combustor exit velocity is inversely proportional to the mass ratio for constant-pressure mixing and burning (eq. (8), Method of Analysis section). Increasing mass ratios therefore lower the combustor exit velocity and Mach number. This is seen in figure 3. Supersonic velocities are possible only at low mass ratios--below 2. Also, since increasing the drive rocket chamber pressure increases the drive gas velocity, the combustor exit velocity and Mach number is also increased as seen in figure 3(a). This effect however is small at the higher mass ratios but is more significant at mass ratios less than 2. In figure 3(b) the combustor exit Mach numbers are seen to increase with decreasing drive rocket static pressure. This follows also from the increase in drive gas velocity with decreasing static pressure. Figure 3 shows therefore that supersonic velocities are possible at the combustor exit, but only at low mass ratios. Large changes in drive rocket chamber pressure and static pressures result in only a small increase in the mass ratios for which supersonic velocities can be sustained.

Figure 4 shows the effects of mass ratio and drive rocket chamber pressure and static pressure on vacuum specific impulse. At zero mass ratio the vacuum impulse is that corresponding to a conventional rocket with the same chamber pressure as the drive rocket. Small increases in mass ratio decrease the specific impulse sharply. At mass ratios above 2 or 3 the impulse remains approximately constant and is the impulse that would be obtained from a conventional rocket having a chamber pressure equal to the drive rocket static pressure. It follows therefore that decreasing static pressures result in decreasing impulses as shown in figure 4. Higher drive rocket chamber pressures improve the specific impulse only at the lower mass ratios. In figure 4 the dashed curve is for a drive rocket chamber pressure of 200 atmospheres and nozzle exit pressure of 3 atmospheres. At a zero mass ratio (conventional rocket) the specific impulse is 16 seconds higher; however at a mass ratio of only 2, the specific impulse improvement for the higher chamber pressure is only 5 seconds. At mass ratios greater than 5 little improvement in performance results from higher chamber pressures.

Variable Pressure Mixing and Burning

Increasing the combustor area ratio and decreasing the pressure results in higher combustor exit Mach numbers and improved performance. This is shown in figures 5(a) and 5(b) for a mass ratio of 10 assuming

a linear pressure distribution in the combustor. Indicated in the figures are the combustor exit Mach number and specific impulse for constant pressure mixing and burning which results in an area ratio of 20. It is seen from the figures that the supersonic solution for an area ratio of 20 yields a lower specific impulse than for the constant pressure process. Increasing the combustor area ratio, however, results in a rapid increase in specific impulse from 400 seconds at an area ratio of 20 to 481 seconds at an area ratio of 38.5. As indicated, this performance equals that of a conventional rocket with the same chamber pressure as the drive rocket.

Effect of combustor pressure distribution. - As mentioned before, three pressure profiles are considered (fig. 2). The effect of these profiles on vacuum specific impulse is shown in figure 6. It is seen that for successively lower pressure distributions ranging from the linear profile to the elliptic profile larger combustor area ratios are required to obtain a specified vacuum specific impulse. It is also noted in figure 6, that values of specific impulse for the three pressure profiles exceed that attainable by a conventional rocket having the same chamber pressure as the drive rocket and expanded to a nozzle exit pressure of 0.01 atmosphere. The maximum specific impulse that can be calculated is for the case when all thermal energy is converted to kinetic energy. That is when either the combustor exit temperature or nozzle exit temperature is zero. The minimum combustor exit temperature considered for the curves in figure 6 is 20 K (36° R), which results in a specific impulse approaching the maximum value of 531 seconds. Since the average pressure profile assumes the most efficient conversion of thermal energy to kinetic energy of the three profiles, the maximum impulse is approached with the smallest combustor area ratio. Or stated another way, for the same combustor area ratio an average pressure profile results in a higher combustor exit velocity and lower temperature than for the lower profiles. Thus, for example, the area ratio required for a combustor exit temperature of 20 K (36° R) is 48 compared to 116 for the elliptic profile. For all profiles assumed, however, the maximum impulse equals that of a conventional rocket for a nozzle expansion to an exit temperature of 20 K (36° R). This of course follows from conservation of energy, since the thermal energy is the same for both the conventional rocket and supersonic-burning rocket.

For a nozzle expansion to a finite pressure of 0.0λ atmosphere (fig. 5(b)) the specific impulse is related to the combustor exit total pressure. Therefore a specific impulse higher than that attainable by a conventional rocket with the same chamber pressure as the drive rocket suggests a combustor exit total pressure higher than that of the drive rocket. For example, from figure 5(b) the combustor area ratio of 38.5 results in a specific impulse of 481 seconds for the linear combustor pressure distribution. The same specific impulse is obtained by a conventional rocket with a chamber pressure of 50 atmospheres. It is seen from figure 7(a) that, for this combustor area ratio, the combustor exit pressure is 50 atmospheres and that higher area ratios result in total pressures higher than that of the drive rocket. This

same phenomenon was observed in reference 1 and is explained as follows. It is well known that a simple cooling process decreases the entropy of a gas and increases the total pressure whereas heat addition increases entropy and decreases total pressure. Since the total temperature of the oxygen and hydrogen entering the combustor are much less than that of the gas leaving the combustor, the entropy of the gas must be higher than the mass weighted entropy of the three streams entering the combustor. Otherwise a violation of the second law of thermodynamics is indicated. Figure 7(b) shows the computed ratio of combustor exit entropy to the mass-weighted combustor entrance entropy versus combustor area ratio. It is seen that the entropy ratios are always greater than one, even for the area ratios where the combustor exit total pressures are greater than the drive rocket chamber pressure. Thus, contrary to the simple heating case mentioned previously, we apparently have the situation of both entropy and total pressure increasing with heat addition. However it should be borne in mind that the present analysis considers only the initial and final temperatures of the combustor. Temperature distributions within the combustor are not considered explicitly, but instead are implicitly defined through the assumed wall pressure profile. Thus, it is possible that it may require a complex and impractical combination of heating and cooling processes to obtain the computed increase in total pressure above that of the drive rocket. Inasmuch as the present study does not consider the situation in more detail, for conservatism the remaining discussion is limited to cases for which the combustor exit total pressure is no greater than that of the drive rocket chamber pressure. Also the parabolic profile was used for the combustor pressure distribution for the remaining parametric results.

Effect of mass ratio. - Figure 8 shows the effect of mass ratio on vacuum specific impulse and combustor area ratio. The specific impulse increases with increasing combustor area ratios for all mass ratios considered. To obtain the same specific impulse combustor area ratios increase rapidly with mass ratio up to a mass ratio of 10. Above a mass ratio of 20 the combustor area ratios increase only slightly with mass ratio. This may indicate the ejector action of the drive rocket becomes less significant at high mass ratios. However, combustor exit Mach numbers are still supersonic at the high mass ratios. Figure 9 shows the effect of mass ratio on nozzle area ratio. For a specified mass ratio, combustor exit temperatures and pressures decrease with increasing area ratio. Therefore for the fixed nozzle exit pressure of .01 atmospheres less nozzle expansion is required as combustor area ratios increase. Comparing figures 8 and 9 for a given mass ratio, the nozzle area ratios are seen to decrease with increasing specific impulse and combustor area ratios. It is also seen in figure 9 that nozzle area ratios decrease with increasing mass ratio. Since increasing mass ratios result in increasing combustor area ratios and lower combustor exit pressures and temperatures less nozzle expansion is required.

Effects of drive rocket nozzle exit pressure and chamber pressure. - Figures 10 and 11 show the effect of drive rocket nozzle exit pressure

on vacuum specific impulse and combustor and nozzle area ratios. It is seen in figure 10 that to obtain the same specific impulse, combustor area ratios decrease with increasing drive rocket nozzle exit pressures. Since the combustor exit pressures decrease with decreasing drive rocket nozzle pressure, less main rocket nozzle expansion is required to expand the gas to .01 atmospheres. This is seen in figure 11 where the main rocket nozzle area ratios decrease with decreasing drive rocket nozzle exit pressures.

Figure 12 shows that combustor area ratios increase with increasing drive rocket chamber pressure to obtain the same specific impulse. Also since these results are restricted to performance levels no higher than that comparable to the drive rocket chamber pressure the vacuum specific impulse would increase with increasing drive rocket chamber pressure. In figure 13 it is seen that drive rocket chamber pressure has little effect on the main rocket nozzle area ratio. Thus, combustor exit pressures and temperatures are dependent mainly on combustor area ratio and drive rocket nozzle exit pressure.

Parametric Effect on Weight Flow Per Unit Nozzle Exit Area

Although the previous discussion of parametric results show the effects of the various parameters on specific impulse and combustor and nozzle area ratios, the effects on engine size are better illustrated by the total weight flow per unit nozzle exit area. For the same specific impulse a lower weight flow per unit area would indicate a smaller engine and possible lower weight. This would also make comparisons of this concept with conventional rocket engines more meaningful. Figure 14 shows the variation of vacuum specific impulse with weight flow per unit nozzle exit area for the range of mass ratios, combustor area ratios and drive rocket chamber and nozzle exit pressures considered in this study. Also noted in the figure is the variation of specific impulse with combustor exit total pressure. Since a single curve results, the variation of specific impulse with weight flow per unit area is independent of mass ratio and drive rocket nozzle exit pressure and is dependent on combustor area ratio or combustor exit total pressure (fig. 7(a)). Also since combustor exit pressures were limited to values no larger than drive rocket chamber pressures figure 14 can be regarded as the variation of specific impulse and weight flow per unit area with drive rocket chamber pressure. It may be added that figure 14 would be identical to that for a conventional rocket where the conventional rocket chamber pressure would be substituted for the combustor exit total pressures indicated in the figure.

Some of the calculated physical characteristics for a supersonic burning rocket with a vacuum thrust of 896 kN (200 000 lbf) are given in Table III. The combustor exit total pressure is equal to the drive rocket chamber pressure of 50 atmospheres. Therefore the vacuum specific

impulse and nozzle exit area are the same as for a conventional rocket of 896 kN (200 000 lbf) thrust and chamber pressure of 50 atmospheres. In fact, if combustor exit total pressure equal to the drive rocket chamber pressure can be attained the maximum diameter of the supersonic burning rocket would be about the same as a conventional rocket. However, a lighter-weight engine may be possible since turbopumps are eliminated and combustor-exit static temperatures are lower, 1990 K (3580° R) compared to 3600 K (6480° R) for a conventional rocket. In addition, a sonic throat is not required therefore severe cooling problems of the conventional rocket throat are eliminated.

CONCLUDING REMARKS

A preliminary analysis has been made of a supersonic-combustion rocket engine concept for hydrogen and oxygen propellants. This concept features a small drive rocket for pumping the propellants into the combustor thereby replacing conventional turbopumps. Also the burned gas leaves the combustor at a supersonic speed and a sonic throat in the nozzle is not required. Therefore, complicated, heavy turbopumps are eliminated and cooling problems generally severe for the sonic throat of conventional rockets would not be present.

Cycle parameters were varied to determine their effect on the vacuum specific impulse. These parameters include the mass ratio (ratio of mass flow of main rocket propellants to the drive rocket mass flow), the drive rocket chamber and nozzle exit pressure, the combustor area ratio and pressure distribution. The vacuum specific impulse was calculated for a nozzle expansion from the combustor exit pressure to 0.01 atmospheres. The combustor area ratio was found to have the most significant effect on engine performance. The specific impulse increased with increasing combustor area ratios attaining values higher than those attainable with a conventional rocket with the same chamber pressure as the drive rocket. But a more detailed investigation of the mixing and burning process would have to be made to support this phenomenon.

However, for the same drive rocket chamber pressure the vacuum specific impulse was found to be independent of mass ratio, drive rocket nozzle exit pressure and combustor pressure distribution. Increases in mass ratio and decreases in drive rocket nozzle exit pressure required increased combustor area ratio to achieve the same specific impulse.

Decreasing the combustor pressure distribution required increasing the combustor area ratio to obtain the same performance. However the possibility of pressure distributions lower than those considered in this study is admitted.

Attaining specific impulse levels equal to those of a conventional

rocket with the same chamber pressure as the drive rocket makes this concept especially attractive for a low-thrust high-altitude operation in a pressure-feed system. This would result in reduced engine development and weight since no turbopumps are required. Also since only a small part of the total propellant is required for the drive rocket, separate tanks could be used for the drive rocket propellants and the main propellants could be stored at lower pressures and reduced tank weight. However this concept may not be as attractive for low-altitude, high-thrust operation. Since supersonic velocities and low pressures at the combustor exit are required to achieve performance levels comparable to conventional rockets high back pressures at low altitude operation may result in performance penalties.

Since this study was of an exploratory nature a number of simplifications and assumptions were made. For example shock and friction losses were not considered. Also the attractive results of this study are dependent upon regulating the mixing and burning process to obtain supersonic velocities at the combustor exit. The effects of this mixing and burning process on the combustor pressure distribution would have to be investigated. Since one of the significant advantages of this concept lies in pumping large quantities of propellant with a small drive rocket the effect of increasing mass ratios on the mixing and burning would also have to be studied.

REFERENCES

1. Franciscus, Leo C.: Analysis of Rocket-Powered Ejectors for Pumping Liquid Oxygen and Liquid Hydrogen. NASA TN D-6033, 1970.

2. Franciscus, Leo C.; and Healy, Jeanne A.: Computer Program for Determining Effects of Chemical Kinetics on Exhaust-Nozzle Performance. NASA TN D-4144, 1967.

TABLE I. PARAMETER CONSIDERED IN THE STUDY

Parameter	Range of Values
Mass ratio, $\dot{m}_S/\dot{m}_P$	1 - 25
Drive rocket chamber pressure, P_{TP}, atm.	4 - 200
Drive rocket nozzle exit pressure, P_P, atm.	1 - 3
Combustor area ratio, A_2/A_1	10 - 150
Combustor pressure distribution	Average Parabolic Elliptic

TABLE II. - VELOCITIES AND MACH NUMBERS OF DRIVE ROCKET GAS, OXYGEN, AND HYDROGEN ENTERING THE COMBUSTOR

P_{TP}, atm	P_P, atm	M_P	V_P, m/S (ft/sec)	M_H	V_H, m/S (ft/sec)	V_O, m/S (ft/sec)
200	3	3.15	3620 (11 850)	0.68	81 (265)	14 (46)
	2	3.27	3750 (12 300)	1.06	126 (413)	19 (62)
	1	3.58	3950 (12 950)	1.57	168 (550)	23 (75)
100	3	2.76	3360 (11 000)	.68	81 (265)	14 (46)
	2	2.95	3500 (11 480)	1.06	126 (413)	19 (62)
	1	3.26	3750 (12 300)	1.57	168 (550)	23 (75)
50	3	2.42	3040 (9 950)	.68	81 (265)	14 (46)
	2	2.62	3210 (10 500)	1.06	126 (413)	19 (62)
	1	2.95	3480 (11 400)	1.57	168 (550)	23 (75)
4	2	1.14	1540 (5 050)	1.06	126 (413)	19 (62)
	1	1.64	2140 (7 000)	1.57	168 (550)	23 (75)

TABLE III. - PHYSICAL CHARACTERISTICS OF A SUPERSONIC BURNING ROCKET WITH A VACUUM THRUST OF 896 kN

Drive rocket chamber pressure, atm	50
Drive rocket nozzle exit pressure, atm	3
Mass ratio	10
Drive rocket propellant, kg/sec (lbm/sec)	17.1 (380)
Main propellant, kg/sec (lbm/sec)	171 (3800)
Combustor exit temperature, K (^{o}R)	1990 (3580)
Combustor exit pressure, atm	0.0525
Combustor exit Mach number	4.43
Nozzle exit temperature, K (^{o}R)	1472 (2650)
Nozzle exit pressure	0.01
Nozzle exit Mach number	5.04
Drive rocket nozzle exit diameter, m (ft)	0.182 (0.6)
Combustor entrance diameter, m (ft)	0.39 (1.28)
Combustor exit diameter, m (ft)	2.98 (9.8)
Nozzle exit diameter, m (ft)	5.56 (18.25)

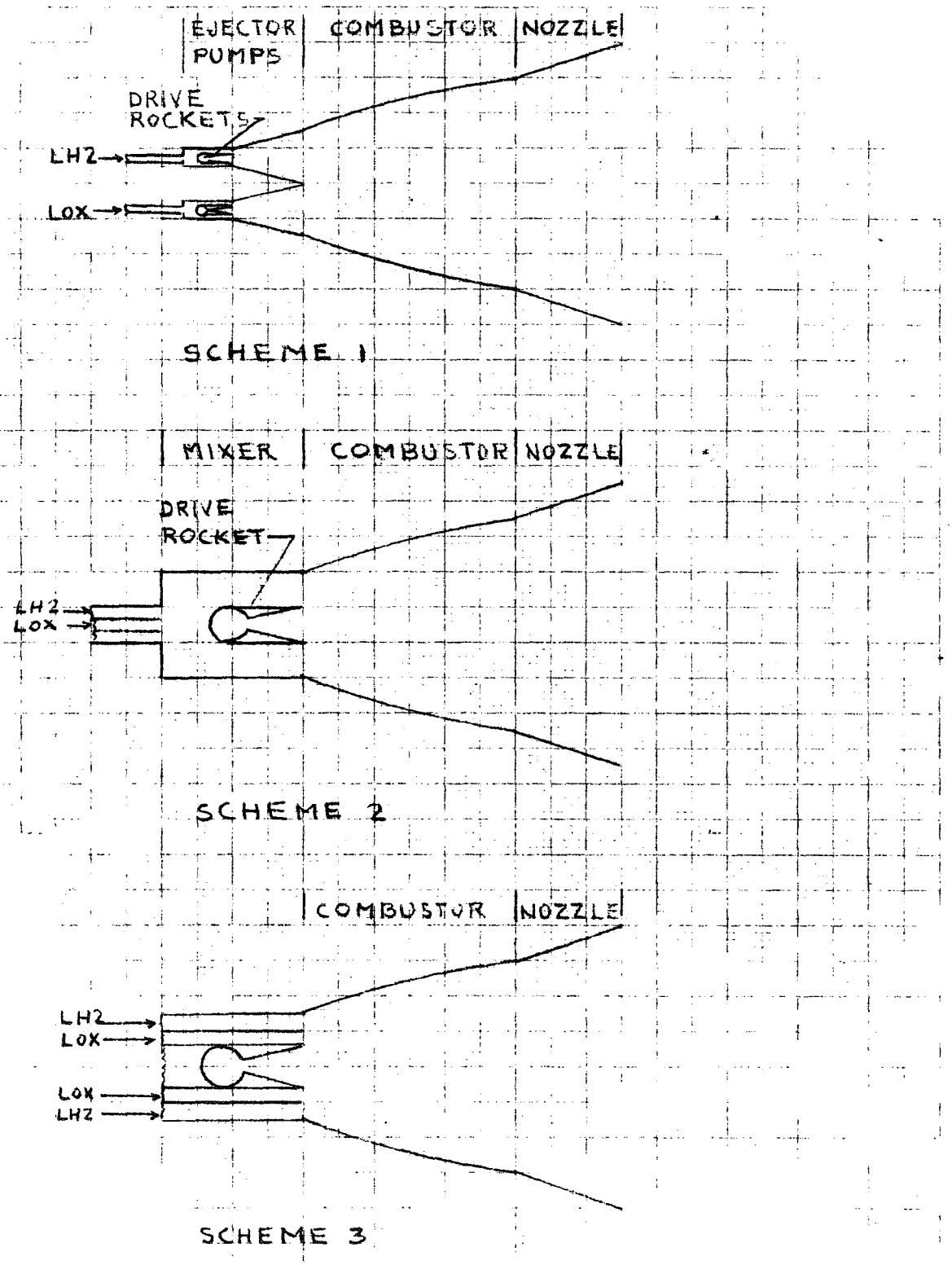

Figure 1. - Schematics of a Supersonic Combustion Rocket

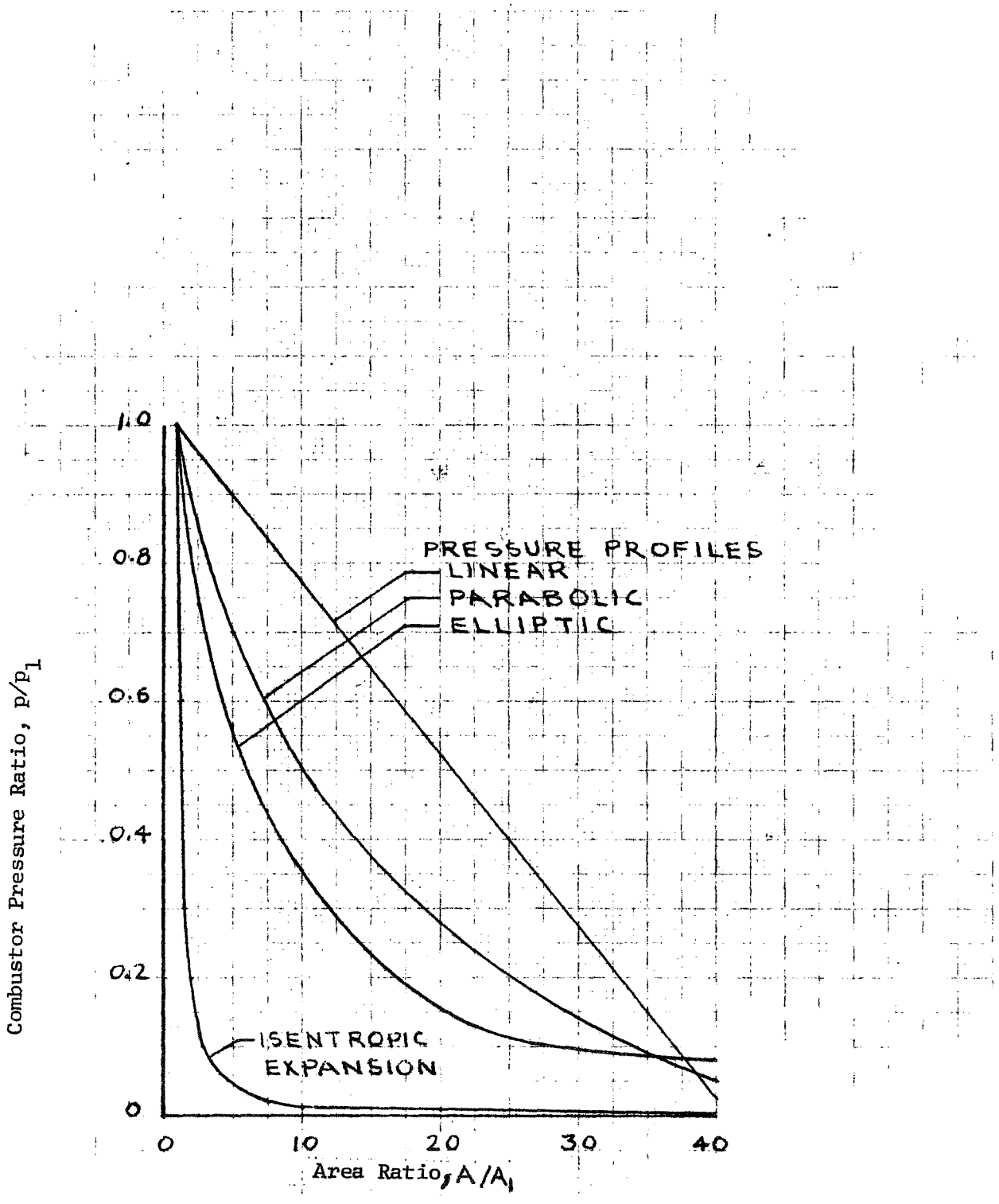

Figure 2. - Typical Pressure Profiles Assumed for Combustor Pressure Distribution

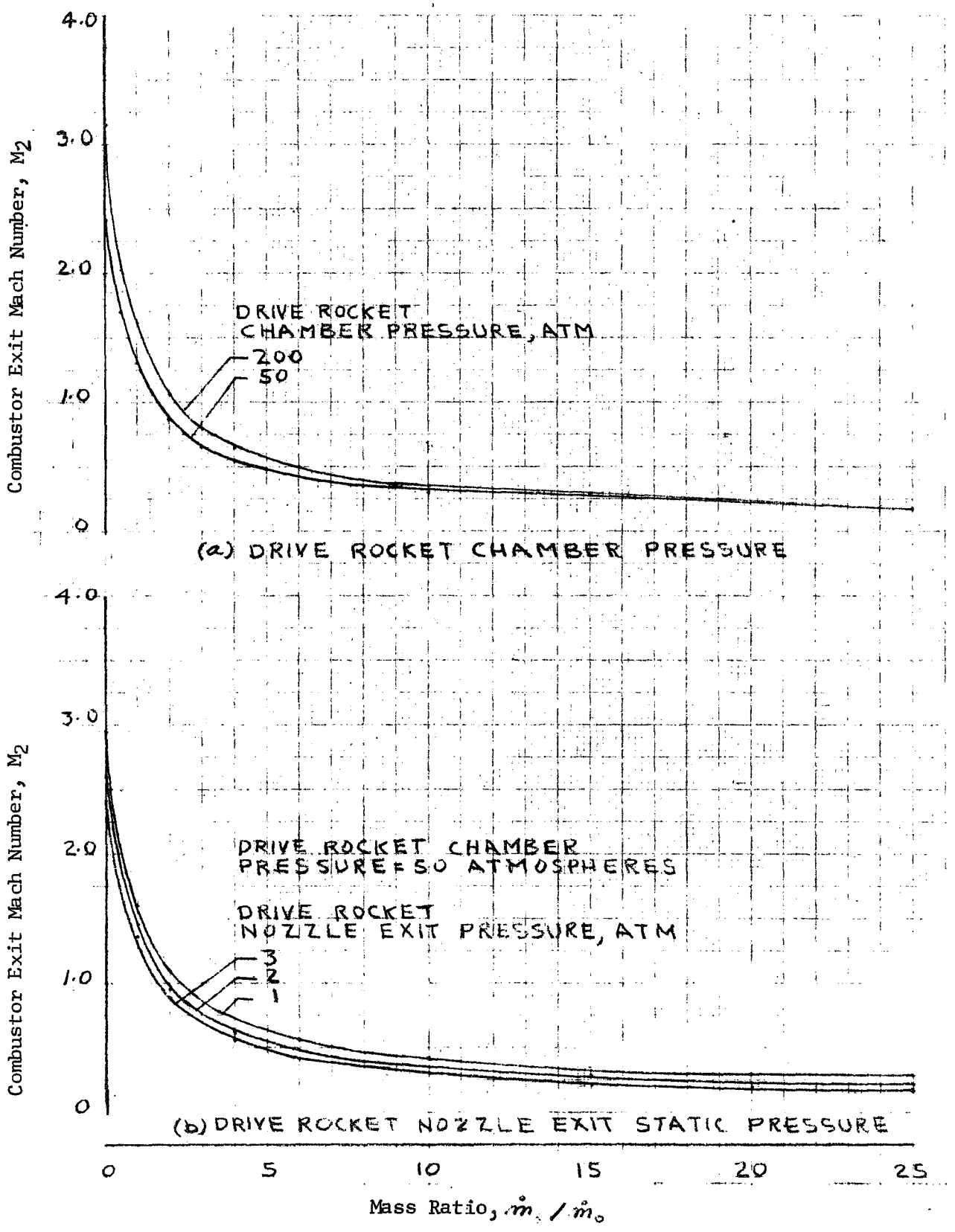

Figure 3. - Effect of Mass Ratio, Drive Rocket Chamber Pressure and Nozzle Exit Static Pressure on Combustor Exit Mach Number for Constant Pressure Combustion.

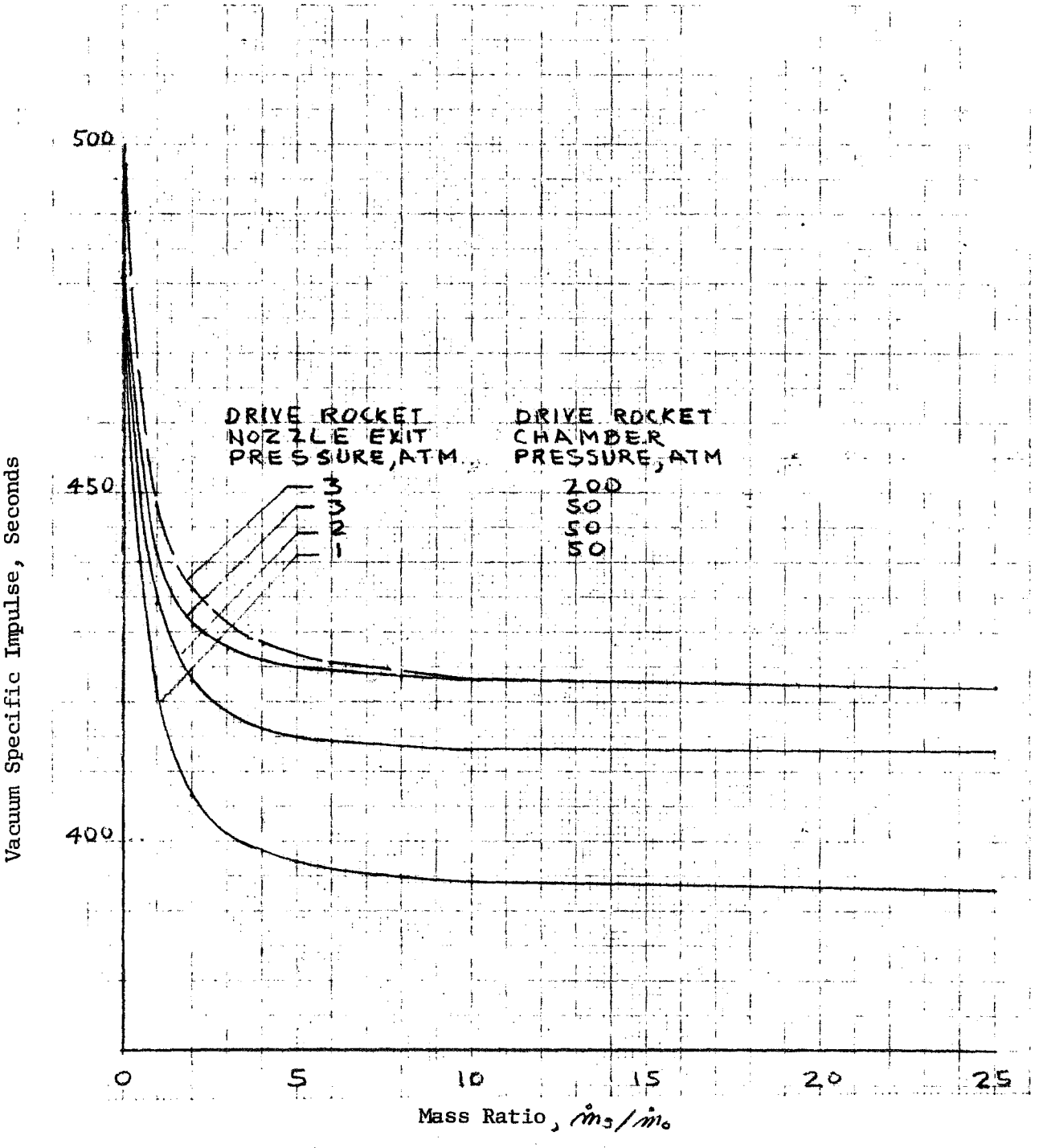

Figure 4. - Effect of Mass Ratio and Drive Rocket Chamber and Nozzle Exit Static Pressures on Vacuum Specific Impulse for Constant Pressure Combustion. Supersonic Combustion Rocket Nozzle Exit Static Pressure, .01 Atm.

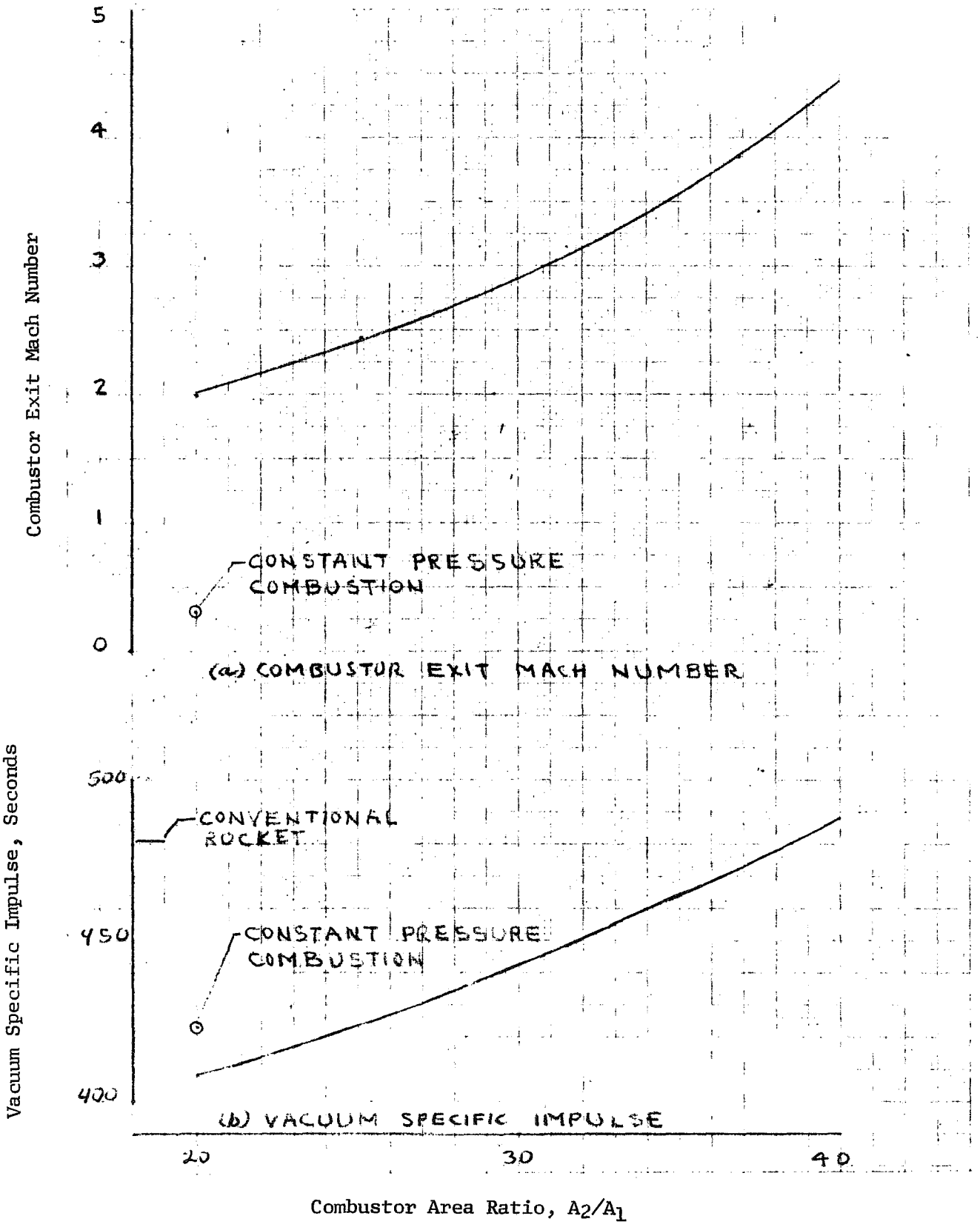

Figure 5. - Effect of Combustor Area Ratio on Combustor Exit Mach Number and Vacuum Specific Impulse. Drive Rocket Chamber Pressure, 50 Atm.; Drive Rocket Nozzle Exit Pressure, 3 Atm.; Mass Ratio, 10; Nozzle Exit Pressure, .01 Atm. Average Combustor Pressure Distribution.

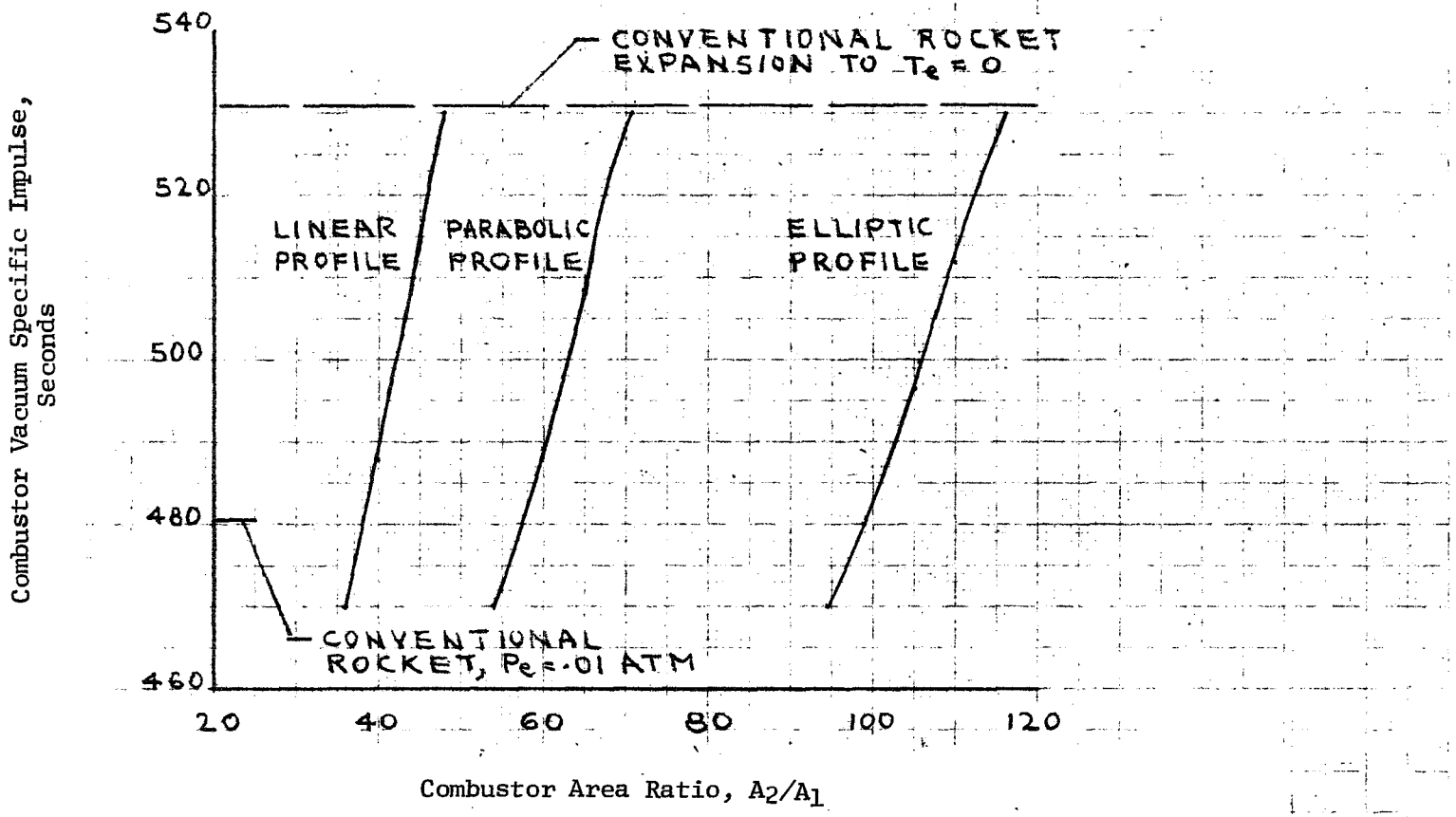

Figure 6. - Effect of Combustor Pressure Distribution on Combustor Area Ratio and Vacuum Specific Impulse. Drive Rocket Chamber Pressure, 50 Atm.; Drive Rocket Nozzle Exit Pressure, 3 Atm.; Mass Ratio, 10.

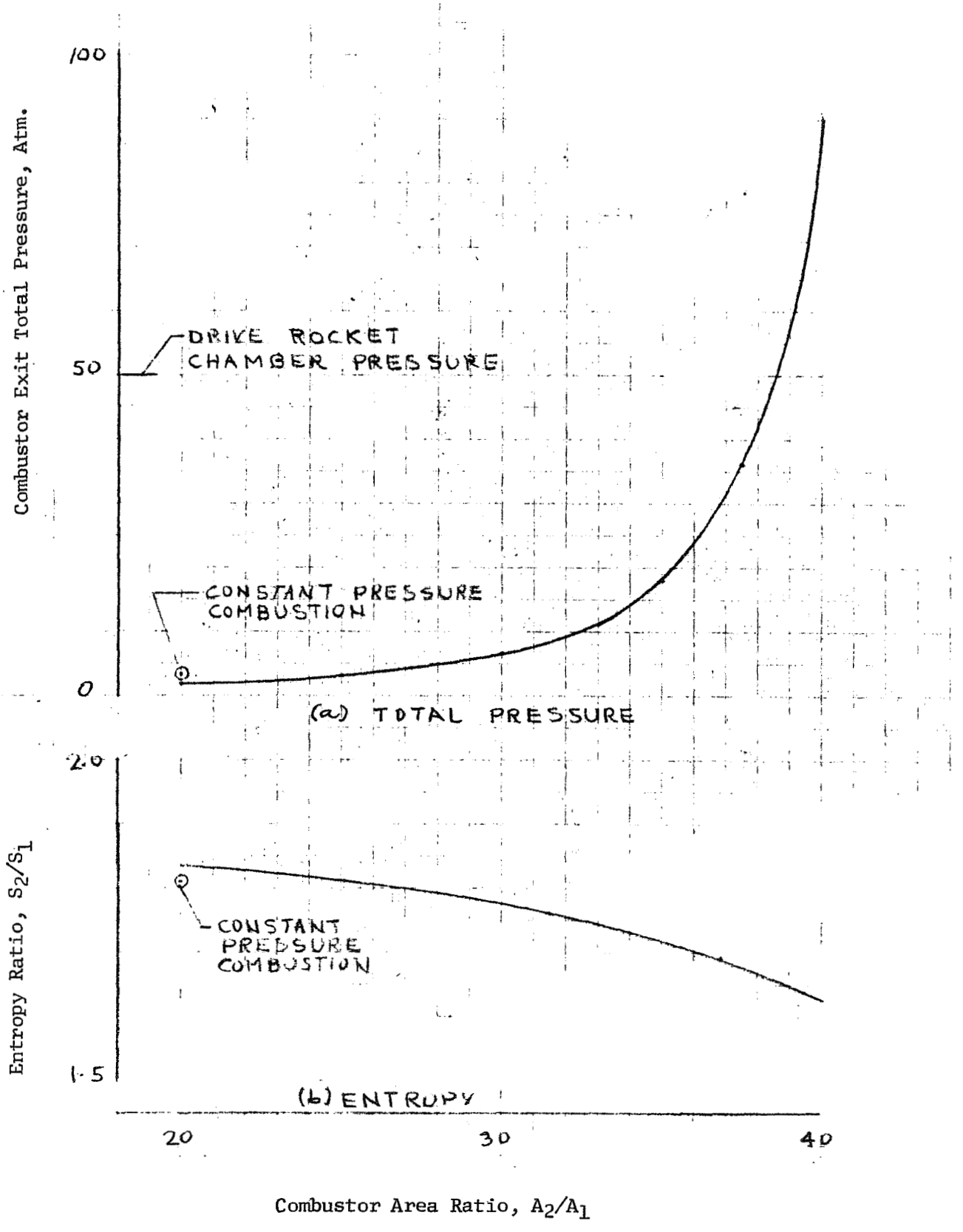

Figure 7. - Effect of Combustor Area Ratio on Combustor Exit Total Pressure and Entropy. Drive Rocket Chamber Pressure, 50 Atm.; Drive Rocket Nozzle Exit Pressure, 3 Atm.; Mass Ratio, 10; Average Combustor Pressure Distribution.

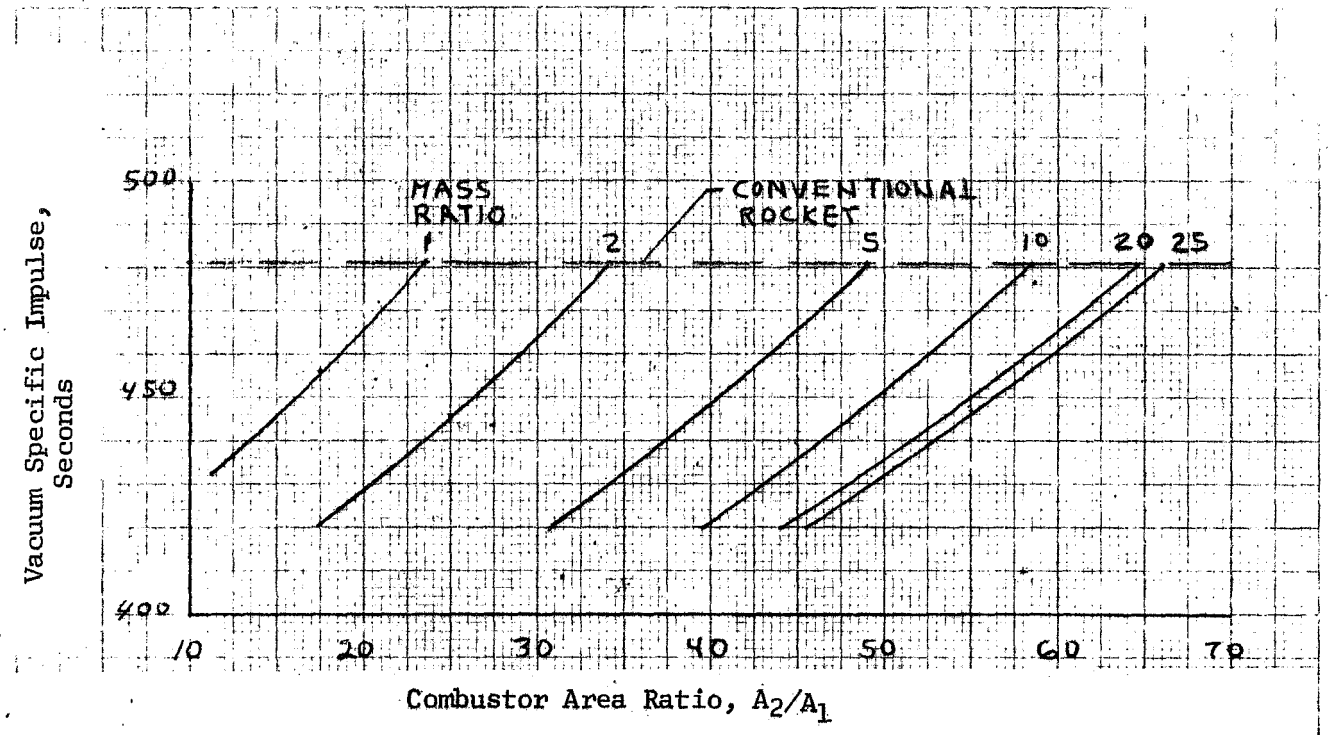

Figure 8. - Effect of Mass Ratio and Combustor Area Ratio on Vacuum Specific Impulse. Nozzle Exit Pressure, .01 Atm.; Drive Rocket Chamber Pressure, 50 Atm.; Drive Rocket Nozzle Exit Pressure, 3 Atm.

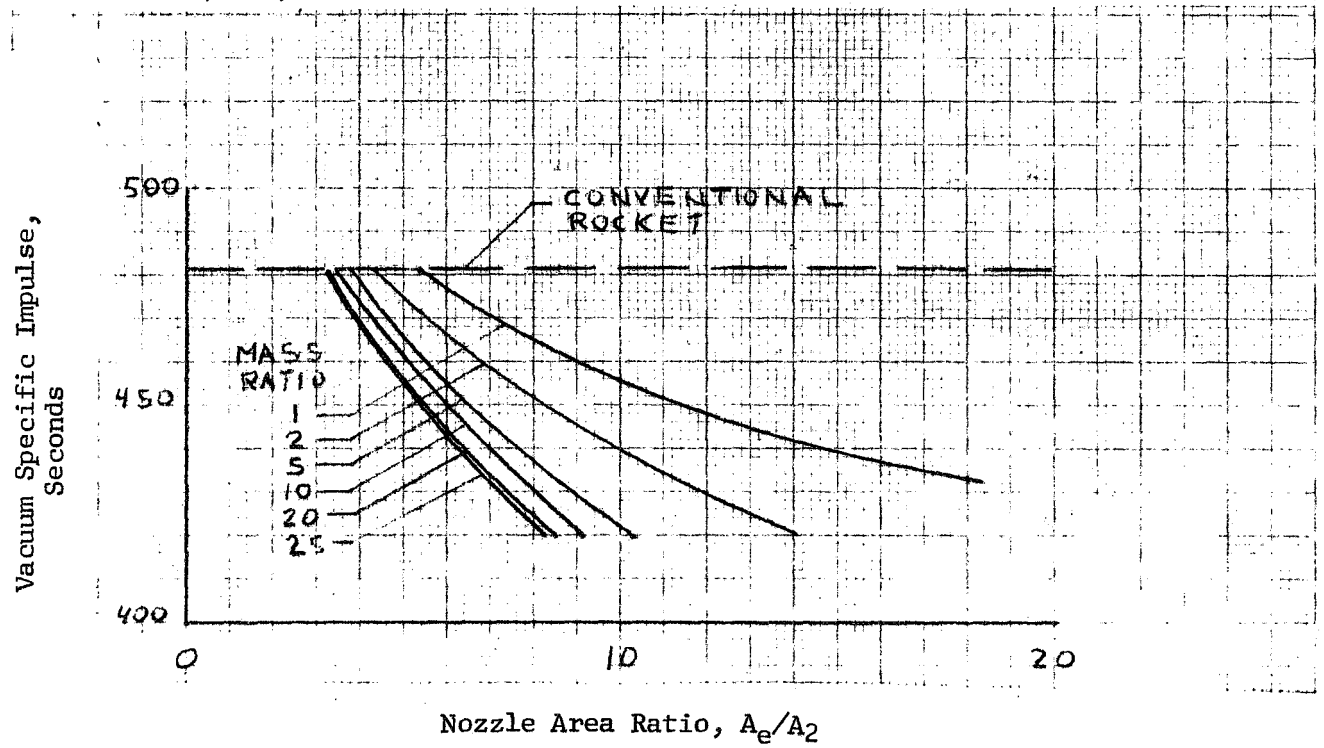

Figure 9. - Effect of Mass Ratio on Vacuum Specific Impulse and Nozzle Area Ratio. Nozzle Exit Pressure, .01 Atm. Drive Rocket Chamber, 50 Atm.; Drive Rocket Nozzle Exit Pressure, 3 Atm.

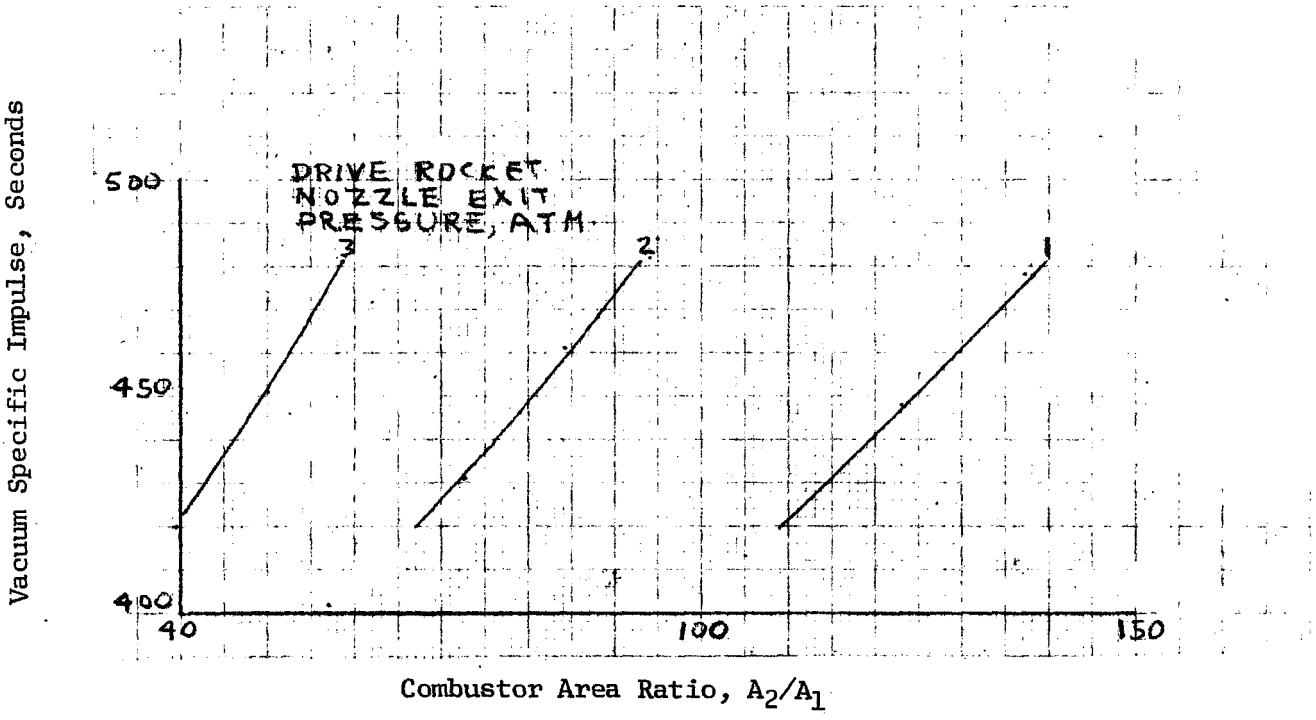

Figure 10. - Effect of Drive Rocket Nozzle Exit Pressure on Vacuum Specific Impulse and Combustor Area Ratio. Drive Rocket Chamber Pressure, 50 Atm.; Nozzle Exit Pressure, .01 Atm.; Mass Ratio, 10.

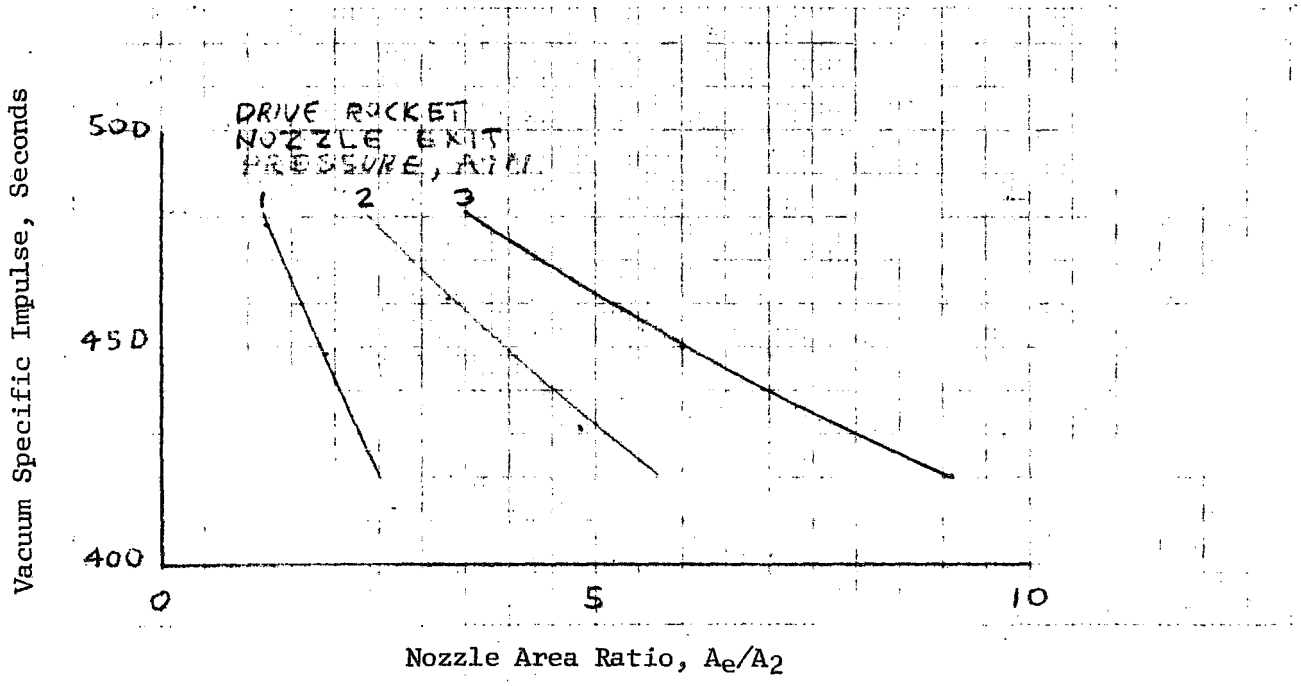

Figure 11. - Effect of Drive Rocket Nozzle Exit Pressure on Vacuum Specific Impulse and Nozzle Area Ratio. Drive Rocket Chamber Pressure, 50 Atm.; Nozzle Exit Pressure, .01 Atm.; Mass Ratio, 10.

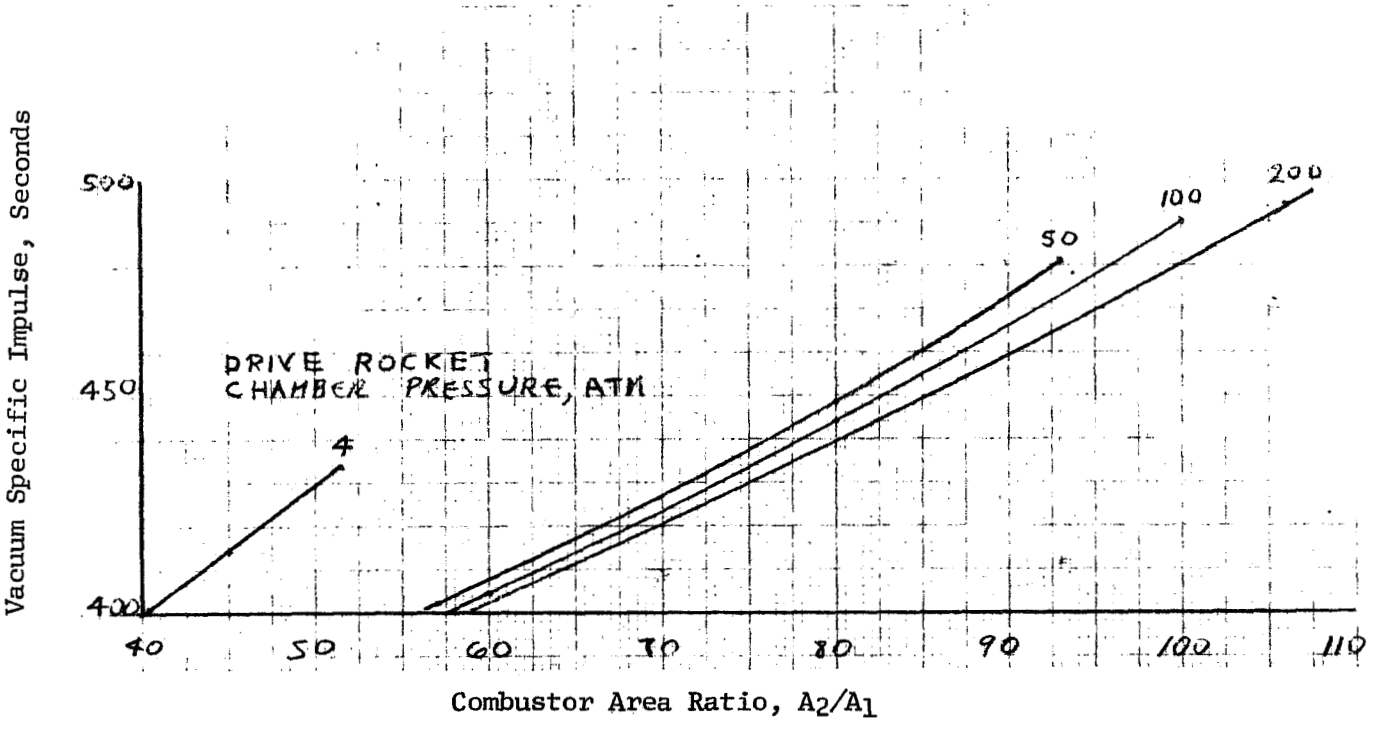

Figure 12. - Effect of Drive Rocket Chamber Pressure on Vacuum Specific Impulse and Combustor Area Ratio. Drive Rocket Nozzle Exit Pressure, 2 Atm.; Mass Ratio, 10.

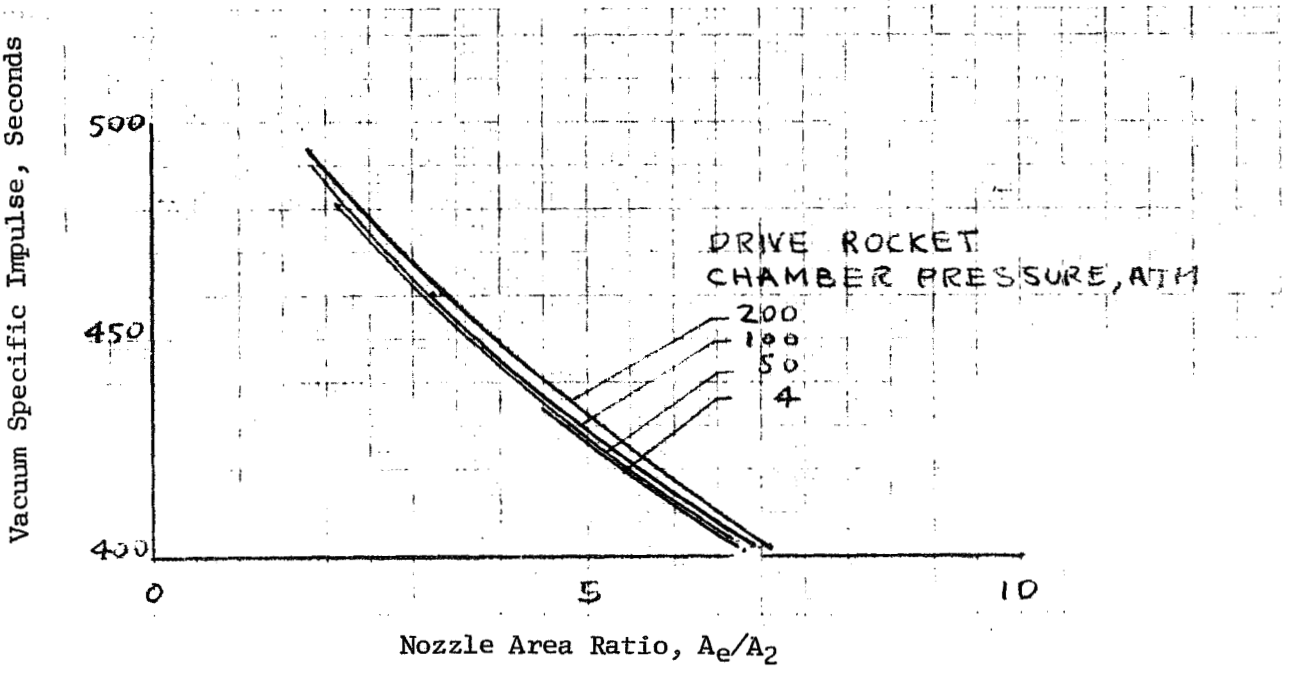

Figure 13. - Effect of Drive Rocket Chamber Pressure on Vacuum Specific Impulse and Nozzle Area Ratio. Drive Rocket Nozzle Exit Pressure, 2 Atm.; Mass Ratio, 10.

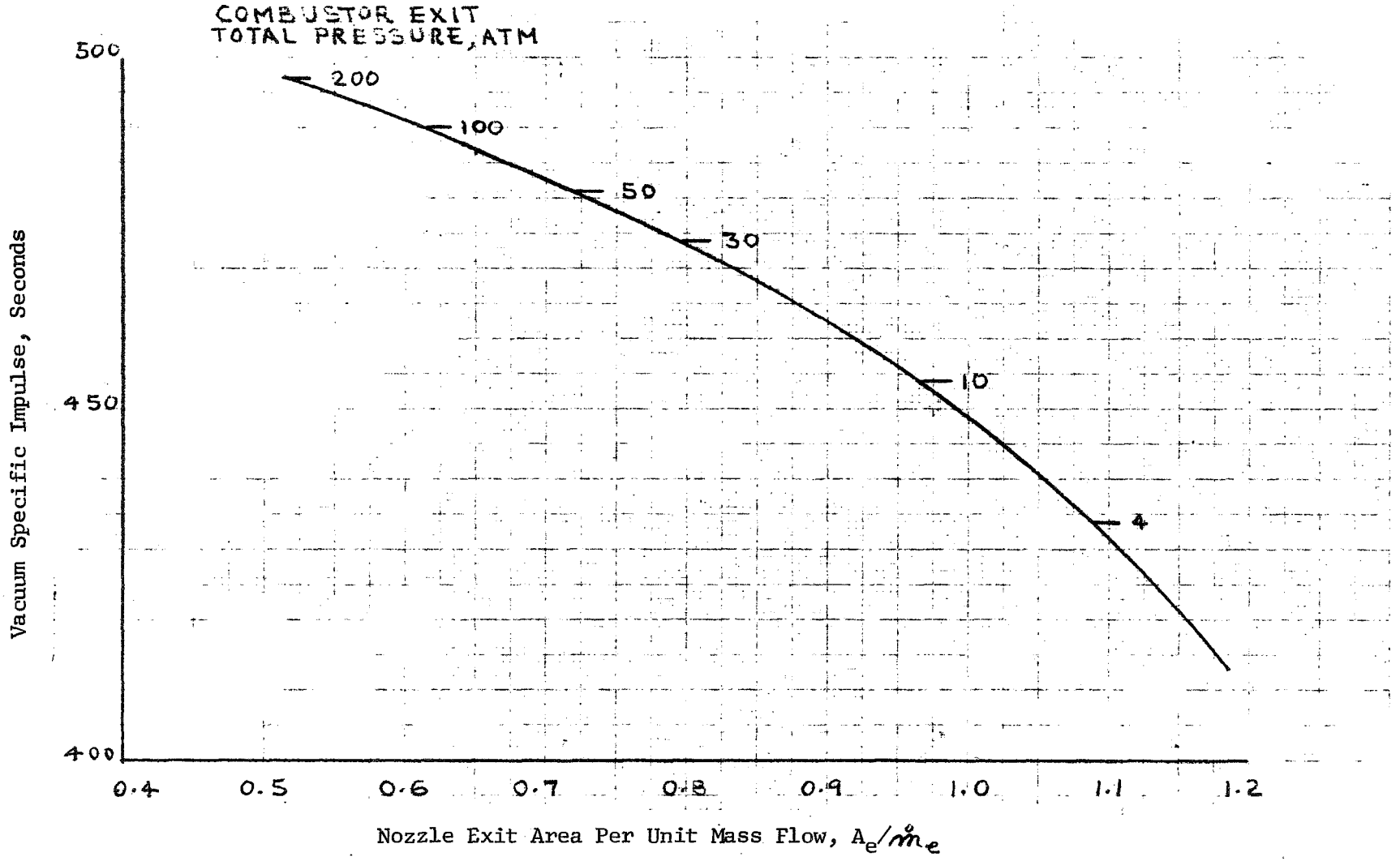

Figure 14. - Variation of Vacuum Specific Impulse and Nozzle Area Per Unit Weight Flow With Combustor Exit Total Pressure. Drive Rocket Chamber Pressures, 4-200 Atm.; Drive Rocket Nozzle Exit Pressures, 1-3 Atm.; Mass Ratios, 1-25; Combustor Pressure Distributions, Linear, Parabolic, Elliptic.